

# Measurement of the branching fractions of radiative leptonic $\tau$ decays $\tau \rightarrow l\gamma\nu\bar{\nu}$ , ( $l = e, \mu$ ) at *BABAR*

Benjamin Oberhof<sup>a,b</sup>,  
on behalf of the *BABAR* collaboration

<sup>a</sup>*Dipartimento di Fisica Università di Pisa, Pisa, Italy*

<sup>b</sup>*Laboratori Nazionali dell'INFN, Frascati, Italy*

---

## Abstract

We perform a measurement of the branching fractions for  $\tau \rightarrow l\gamma\nu\bar{\nu}$ , ( $l = e, \mu$ ) decays for a minimum photon energy of 10 MeV in the  $\tau$  rest frame using  $430 \text{ fb}^{-1}$  of  $e^+e^-$  collisions collected at the center-of-mass energy of the  $\Upsilon(4S)$  resonance with the *BABAR* detector at the PEP-II storage rings. We find  $\mathcal{B}(\tau \rightarrow \mu\gamma\nu\bar{\nu}) = (3.69 \pm 0.03 \pm 0.10) \times 10^{-3}$  and  $\mathcal{B}(\tau \rightarrow e\gamma\nu\bar{\nu}) = (1.847 \pm 0.015 \pm 0.052) \times 10^{-2}$  where the first quoted error is statistical and the second is systematic. These results represent a substantial improvement with respect to existing measurements for both channels.

*Keywords:* Tau lepton, Tau Decays, Tau Properties

---

Leptonic  $\tau$  decays are generally well suited to investigate the Lorentz structure of electroweak interactions in a model-independent way [1]. Leptonic radiative decays  $\tau \rightarrow l\gamma\nu\bar{\nu}$ , ( $l = e, \mu$ ), in particular, have been studied for a long time [2] because they are sensitive to the anomalous magnetic moment of the  $\tau$  [3]. Currently, the branching fraction of the  $\tau \rightarrow e\gamma\nu\bar{\nu}$  decay has been measured only by the CLEO collaboration [4] using  $4.68 \text{ fb}^{-1}$  of  $e^+e^-$  collisions. For a minimum photon energy  $E_{\gamma, \text{min}} = 10 \text{ MeV}$  in the  $\tau$  rest frame they quote the result  $(1.75 \pm 0.06 \pm 0.17) \times 10^{-2}$ , where the first error is statistical and the second systematic. The CLEO collaboration also made the most precise branching fraction measurement of  $\tau \rightarrow \mu\gamma\nu\bar{\nu}$  decay for a minimum photon energy in the  $\tau$  rest frame  $E_{\gamma, \text{min}} = 10 \text{ MeV}$ ,  $(3.61 \pm 0.16 \pm 0.35) \times 10^{-3}$ . In addition, the OPAL collaboration found  $\mathcal{B}(\tau \rightarrow \mu\gamma\nu\bar{\nu}) = (3.0 \pm 0.4 \pm 0.5) \times 10^{-3}$  for a minimum photon energy of 20 MeV in the  $\tau$  rest frame [5]. In the present work, we perform a measurement of  $\tau \rightarrow l\gamma\nu\bar{\nu}$ , branching fractions for a minimum photon energy of 10 MeV in the  $\tau$  rest frame.

This analysis uses data recorded by the *BABAR* detector at the PEP-II asymmetric-energy  $e^+e^-$  storage rings operated at the SLAC National Accelerator Laboratory. The data sample consists of  $431 \text{ fb}^{-1}$  of  $e^+e^-$  collisions recorded at  $\sqrt{s} = 10.58 \text{ GeV}/c$ . The expected cross section for  $\tau$ -pair production is  $\sigma_{\tau\tau} = 0.919 \pm 0.003 \text{ nb}$  [6] corresponding to a data sample of about 400 million  $\tau$ -pairs. A detailed description of the *BABAR* detector is given elsewhere [7]. For this analysis, a Monte Carlo (MC) simulation has been used to estimate the signal efficiency and to optimize the search. Simulated  $\tau$ -pair events are generated using KK2f [9] and  $\tau$  decays are simulated with Tauola [10]. Final-state radiative effects in  $\tau$  decays are simulated using Photos [11]. A  $\tau$ -pair MC sample is generated where each  $\tau$  lepton decays to a mode based on current experimental knowledge [12]. A separate  $\tau$ -pair MC sample is generated where one of the  $\tau$  leptons decays to  $\tau \rightarrow l\gamma\nu\bar{\nu}$ , and the other decays according to known decay modes. We exclude signal events in the former sample to obtain a  $\tau$ -pair background sample. In this article, charge conjugation is always assumed. The MC simulated backgrounds samples include  $\mu^+\mu^-$ ,  $q\bar{q}$  ( $u\bar{u}$ ,  $d\bar{d}$ ,  $s\bar{s}$ ,  $c\bar{c}$ ), and  $B\bar{B}$  ( $B = B^+, B^0$ ) events, where  $\mu^+\mu^-$  events are generated by KK2f [9],  $q\bar{q}$  events are generated using the JETSET generator [13] while  $B\bar{B}$  events are simulated with EVTGEN [14]. The detector response is simulated with GEANT4 [15]. Two-photon and Bhabha backgrounds are estimated directly from the data.

---

*Email address:* benjamin.oberhof@slac.stanford.edu (on behalf of the *BABAR* collaboration)

The signature for  $\tau \rightarrow l\gamma\nu\bar{\nu}$  decays is a charged particle (“track”), identified either as an  $e$  or a  $\mu$  and a neutral deposit in the calorimeter (“cluster”) such that mass and energy of the lepton-photon pair are compatible with that of the parent  $\tau$  lepton. Events with two well-reconstructed tracks and zero total charge are selected, where no track pair is consistent with being a photon conversion in the detector material. The polar angle of each track in the laboratory frame is required to be within the calorimeter acceptance range to ensure a good particle identification. For every track, we require  $p_T > 0.3$  GeV/c and a missing transverse momentum of  $p_{T,miss} > 0.5$  in the event. All neutral clusters are required to have a minimum energy of 50 MeV. We also reject events with neutral clusters with less than 110 MeV if they are closer than 25 cm from a track, where the distance is measured on the inner wall of the EMC.

Each event is divided into hemispheres (signal- and tag- hemisphere) in the center-of-mass (CM) frame by a plane perpendicular to the thrust axis, calculated using all reconstructed charged and neutral particles [16]. The signal hemisphere must contain exactly one track and one neutral cluster. The tag hemisphere must contain exactly one charged track, identified either as an electron, muon or pion, and possibly one additional neutral cluster or  $n\pi^0$  ( $n = 1, 2$ ). Each  $\pi^0$  is built up from a pair of neutral clusters with invariant mass consistent with that of the  $\pi^0$ . To suppress  $e^+e^- \rightarrow \mu^+\mu^-$  and Bhabha events, we reject events in which the signal-side and tag-side leptons have the same flavor. In the signal hemisphere, we require for both channels that the distance between the charged track and the neutral cluster on the inner wall of the EMC is less than 100 cm. For every event, the magnitude of the thrust is required to be within 0.9 and 0.995. The lower limit on the thrust magnitude helps to reject most  $q\bar{q}$  events while the upper limit helps to reject  $e^+e^- \rightarrow \mu^+\mu^-$  and Bhabha events. For the same reason, we impose the total reconstructed energy to be less than 9 GeV.

Electrons are identified applying a multivariate algorithm using as input the ratio of calorimeter energy to the magnitude of the vector momentum of the track ( $E/p$ ), the ionization loss in the tracking system ( $dE/dx$ ), and the shape of the shower in the calorimeter. Muon identification makes use of a bagged decision tree (BDT) algorithm [17], which uses as input the number of hits in the IFR, the number of interaction lengths traversed, and the energy deposition in the calorimeter. Since muons with momenta less than 500 MeV/c do not penetrate into the IFR, the BDT uses also information obtained from the inner trackers to maintain a very low  $\pi - \mu$  misidentification probability with high selection

efficiencies. The electron and muon identification efficiencies are 91% and 62%, respectively. The probability for a  $\pi$  to be misidentified as an  $e$  in  $\tau$  decays is below 0.1%, while the probability to be misidentified as a  $\mu$  is around 1% depending on momentum.

After the preselection, both samples are dominated by background events. For the  $\tau \rightarrow \mu\gamma\nu\bar{\nu}$  sample, the main background sources are  $\tau \rightarrow \mu\nu\bar{\nu}$ ,  $\tau \rightarrow \pi\pi^0\nu$  decays,  $e^+e^- \rightarrow \mu^+\mu^-$  events, and  $\tau \rightarrow \pi\nu$  decays. For the  $\tau \rightarrow e\gamma\nu\bar{\nu}$  sample, almost all background contribution is from  $\tau \rightarrow e\nu\bar{\nu}$  decays in which the electron radiates a photon in the magnetic field of the detector (bremsstrahlung). Further background suppression is obtained by placing requirements on the angle between the lepton and photon in the CM frame ( $\cos\theta_{l\gamma}$ ). For  $\tau \rightarrow \mu\gamma\nu\bar{\nu}$  we require  $\cos\theta_{l\gamma} > 0.99$ , while for  $\tau \rightarrow e\gamma\nu\bar{\nu}$  we require  $\cos\theta_{l\gamma} > 0.97$  (see Figs. 1 and 2). To reject background from  $\tau \rightarrow e\nu\bar{\nu}$  decays in the  $\tau \rightarrow e\gamma\nu\bar{\nu}$  sample, we further impose a minimum value for the invariant mass of the lepton-photon pair  $M_{l\gamma} \geq 0.14$  GeV/ $c^2$  for this channel.

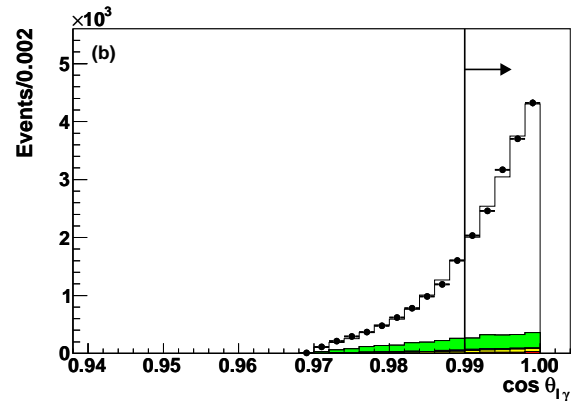


Figure 1: Cosine of the angle between the lepton and photon momenta in the CM frame for radiative  $\tau$  decay into a muon after applying all selection criteria except the one on the plotted quantity. The selection criteria on the plotted quantity are highlighted by the vertical lines; we retain the regions indicated by the horizontal arrow. In green  $\tau \rightarrow \mu\nu\bar{\nu}$  decays, in blue  $\tau \rightarrow \pi\pi^0\nu$  decays, in red  $e^+e^- \rightarrow \mu^+\mu^-$  events, in white signal  $\tau \rightarrow \mu\gamma\nu\bar{\nu}$  decays, and in yellow other (background)  $\tau$ . The black dots are data.

In addition to the afore-mentioned quantities, the selection criteria in both channels use the energy of the photon and the distance between the track and neutral deposit  $d_{l\gamma}$  on the inner EMC wall. The selection criteria are optimized in order to give the smallest statistical and systematic uncertainty on the branching fractions. After optimization, for  $\tau \rightarrow \mu\gamma\nu\bar{\nu}$ , we require  $\cos\theta_{l\gamma} \geq 0.99$ ,  $0.10 \leq E_\gamma \leq 2.5$  GeV,  $6 \leq d_{l\gamma} \leq 30$

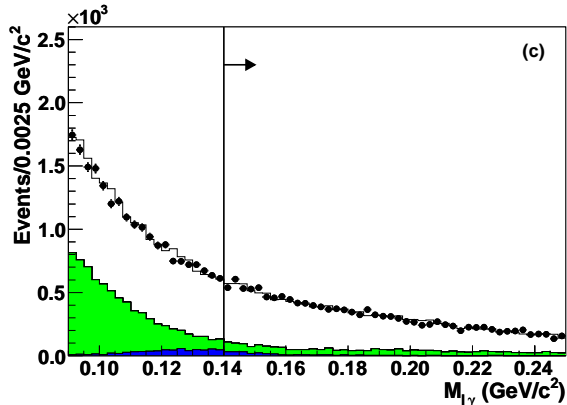


Figure 2: Invariant mass of the lepton photon pair for radiative  $\tau$  decay into an electron after applying all selection criteria except the one on the plotted quantity. The selection criteria on the plotted quantity are highlighted by the vertical lines; we retain the regions indicated by the horizontal arrow. In green  $\tau \rightarrow e\gamma\nu$  decays, in white signal  $\tau \rightarrow e\gamma\nu$  decays, and in blue other (background)  $\tau$ . The black dots are data.

Mode	$\tau \rightarrow \mu\gamma\nu\bar{\nu}$	$\tau \rightarrow e\gamma\nu\bar{\nu}$
Efficiency (%)	$0.480 \pm 0.010$	$0.105 \pm 0.003$
$B/N$	$0.102 \pm 0.002$	$0.156 \pm 0.003$
$N_{exp}$	$15649 \pm 125$	$18115 \pm 135$
$N_{obs}$	15688	18149

Table 1: Signal efficiency, background contribution  $B/N = N_{bkg}/(N_{sig} + N_{bkg})$ , where  $N_{sig}$  are signal and  $N_{bkg}$  background events, number of expected events ( $N_{exp} = N_{sig} + N_{bkg}$ ) and number observed events ( $N_{obs}$ ) for the two decay mode after applying all selection criteria.

cm and  $M_{l\gamma} \leq 0.25$  GeV/ $c^2$ . For the  $\tau \rightarrow e\gamma\nu\bar{\nu}$  channel, we require  $\cos\theta_{l\gamma} \geq 0.97$ ,  $0.22 \leq E_\gamma \leq 2.0$  GeV,  $8 \leq d_{l\gamma} \leq 65$  cm while the lower cut on the invariant mass is set to  $M_{l\gamma} \geq 0.14$  GeV/ $c^2$ . The selection efficiency determined using the MC samples is given in Table 1.

The branching fraction is determined using

$$\mathcal{B}_l = \frac{N_{obs} - N_{bkg}}{2 \sigma_{\tau\tau} \mathcal{L} \epsilon} \quad (1)$$

where  $N_{obs}$  is the number of observed events,  $N_{bkg}$  is the number of expected background events,  $\sigma_{\tau\tau}$  is the cross section for  $\tau$  pair production,  $\mathcal{L}$  is the total integrated luminosity and  $\epsilon$  is the signal efficiency determined from the MC. After applying all selection criteria we find

$$\mathcal{B}(\tau \rightarrow \mu\gamma\nu\bar{\nu}) = (3.69 \pm 0.03 \pm 0.10) \times 10^{-3} \quad (2)$$

$$\mathcal{B}(\tau \rightarrow e\gamma\nu\bar{\nu}) = (1.847 \pm 0.015 \pm 0.052) \times 10^{-2} \quad (3)$$

where the first error is statistical and the second is systematic. Efficiency, background expectations ( $N_{bkg}$ ) and the number of observed events ( $N_{obs}$ ) are shown in Table 1.

Uncertainties on signal efficiency estimation and on the number of the expected background events affect the final result. For background estimation, we define control regions that are enhanced with background events. For  $\tau \rightarrow \mu\gamma\nu\bar{\nu}$ , where the major background contribution is not peaking in  $\cos\theta_{\mu\gamma}$ , we invert the cut on  $\cos\theta_{\mu\gamma}$ . For  $\cos\theta_{\mu\gamma} < 0.8$ , the maximum expected signal rate is 3% of the corresponding background rate. The maximum discrepancy between the MC sample prediction and the number of observed events is 8%, with an excess of events in the MC sample. We take this discrepancy as estimate of the uncertainty on background prediction. For  $\tau \rightarrow e\gamma\nu\bar{\nu}$  whose major background contributions have similar  $\cos\theta_{e\gamma}$  distributions as signal, we apply a similar strategy after requiring the invariant mass  $M_{l\gamma} < 0.14$  GeV/ $c^2$ ; in this case we take  $\cos\theta_{e\gamma} < 0.90$ . The maximum contamination of signal events in this region is 10%, and the maximum discrepancy between the prediction and the number of observed events is 4% with an excess of data events. We take this value as an estimate of the uncertainty on background rate. The error on the branching fractions due to the uncertainty on background estimates are 0.9% for  $\tau \rightarrow \mu\gamma\nu\bar{\nu}$ , and 0.7% for  $\tau \rightarrow e\gamma\nu\bar{\nu}$ , respectively (Table 2). Cross-checks of the background estimation are performed by considering the number of events expected and observed in different sideband regions immediately neighboring the signal region for each decay mode and found to be compatible with the aforementioned systematic uncertainties.

The most important contributions to the error on efficiency come from the uncertainties on particle identification and photon detection efficiency. Uncertainties on particle identification efficiency are estimated on data control samples, by measuring the variation of the data and MC efficiencies for tracks with the same kinematic properties. The uncertainty on the efficiency of the electron identification is evaluated using a control sample consisting of radiative and non-radiative Bhabha events, while the uncertainty for muons is estimated using an  $e^+e^- \rightarrow \mu^+\mu^-\gamma$  control sample. The uncertainty on the pion misidentification probability, as muon or electron, is evaluated using samples of  $\tau \rightarrow \pi\pi\nu$  decays. The corresponding systematic error on the efficiency for  $\tau \rightarrow l\gamma\nu\bar{\nu}$  is 1.5% for both channels. To estimate the uncertainty on photon detection efficiency, we rely on two different processes depending on photon energy: for high energy photons we use  $e^+e^- \rightarrow \mu^+\mu^-\gamma$

	$\tau \rightarrow \mu\gamma\nu\bar{\nu}$	$\tau \rightarrow e\gamma\nu\bar{\nu}$
Selection Criteria	–	2.0
Photon efficiency	1.8	1.8
Particle Identification	1.5	1.5
Background Evaluation	0.9	0.7
PDG BF	0.7	0.7
$N_{\tau\tau}$ $\tau$ pairs	0.6	0.6
MC Statistics	0.5	0.6
Trigger Selection	0.5	0.6
Track Reconstruction	0.3	0.3
Total:	2.8	3.4

Table 2: Summary of systematic contributions to the branching fraction (in relative percent) for the two signal channels.

events while for low energy photons we extract the uncertainty from  $\pi^0$  reconstruction efficiency. In which the photon kinematics can be fully reconstructed using the muon pair. Using fully reconstructed  $e^+e^- \rightarrow \mu^+\mu^-\gamma$  events, data and MC are found to be compatible within 1% for photon energies above 1 GeV. For photon energies below 1 GeV we measure the  $\pi^0$  reconstruction efficiency from the ratio of the branching fractions for  $\tau \rightarrow \pi\nu$  and  $\tau \rightarrow \rho\nu$  decays. The resulting uncertainty on the  $\pi^0$  reconstruction efficiency is found to be below 3%. Including the 1.1% uncertainty on the branching fractions, the resulting uncertainty on single photon detection efficiency is 1.8%. We take this last value as systematic contribution to the efficiency for  $\tau \rightarrow l\gamma\nu\bar{\nu}$  due to photon detection efficiency. Another possible source of systematic uncertainty arises from the choice of the selection criteria; for  $\tau \rightarrow e\gamma\nu\bar{\nu}$  we observe a maximum deviation of 2% from the mean value of the branching fraction depending on the value of  $\cos\theta_{l\gamma}$  used for selection. We take this value as estimate for the uncertainty on the efficiency due to the choice of selection criteria. A similar study on  $\tau \rightarrow \mu\gamma\nu\bar{\nu}$  shows that in this case there is no dependence of the result from selection criteria and thus the corresponding uncertainty is negligible. All other sources of uncertainty in the signal efficiency are found to be smaller than 1.0%, including limited MC statistics, track momentum resolution, observables used in the selection criteria, and knowledge of the tau branching fractions.

In conclusion, we made a measurement of the branching fractions of the radiative leptonic  $\tau$  decays  $\tau \rightarrow e\gamma\nu\bar{\nu}$  and  $\tau \rightarrow \mu\gamma\nu\bar{\nu}$  for a minimum photon energy of 10 MeV in the  $\tau$  rest frame using the full dataset of  $e^+e^-$  collisions collected by *BABAR* at the center-of-mass energy of the  $\Upsilon(4S)$  resonance. We find  $\mathcal{B}(\tau \rightarrow \mu\gamma\nu\bar{\nu}) = (3.69 \pm 0.03 \pm 0.10) \times 10^{-3}$  and  $\mathcal{B}(\tau \rightarrow e\gamma\nu\bar{\nu}) = (1.847 \pm$

$0.015 \pm 0.052) \times 10^{-2}$  where the first error is statistical and the second is systematic. These results represent an improvement of about a factor of three for both channels with respect to the previous experimental bounds [4], reducing both statistic and systematic contributions for both channels. The main contribution to the total error for both measurements comes from the photon detection efficiency and particle identification. For  $\tau \rightarrow e\gamma\nu\bar{\nu}$ , there is also an important contribution coming from the dependence of the final result from the selection criteria on the lower value of the outgoing electron and the photon. Our results are in agreement with the SM values,  $\mathcal{B}(\tau \rightarrow \mu\gamma\nu\bar{\nu}) = (3.686 \pm 0.009) \times 10^{-3}$  and  $\mathcal{B}(\tau \rightarrow e\gamma\nu\bar{\nu}) = (1.843 \pm 0.002) \times 10^{-2}$ , obtained from the TAUOLA [10] MC, which uses the PHOTOS [11] package to simulate QED radiative corrections in the decay up to third order in the fine structure constant  $\alpha$ .

## References

- [1] L. Michel, Proc. Roy. Soc. Lond. A **63**, 514 (1950).
- [2] M. L. Laursen, M. A. Samuel, and A. Sen, Phys. Rev. D **29**, 2652 (1984).
- [3] M. Fael *et al.*, arXiv:1301.5302, (2013).
- [4] T. Bergfeld *et al.* (CLEO collaboration), Phys. Rev. Lett. **84**, 830-834 (2000).
- [5] G. Alexander *et al.* (OPAL collaboration), Phys. Lett. B **388**, 437 (1996).
- [6] S. Banerjee *et al.*, Phys. Rev. D **77**, 054012 (2008).
- [7] B. Aubert *et al.* (*BABAR* collaboration), Nucl. Instrum. Methods Phys. Res., Sect. A **479**, 1 (2002).
- [8] B. Aubert *et al.* (*BABAR* collaboration), Nucl. Instrum. Methods Phys. Res., Sect. A **729**, 615-701 (2013).
- [9] S. Jadach, B. F. Ward, and Z. Was, Comput. Phys. Commun. **130**, 260 (2000).
- [10] S. Jadach *et al.*, Comput. Phys. Commun. **76**, 361 (1993).
- [11] E. Barberio and Z. Was, Comput. Phys. Commun. **79**, 291 (1994).
- [12] K.A. Olive *et al.* (Particle Data Group), Chin. Phys. C, **38**, 090001 (2014)
- [13] T. Sjostrand, S. Mrenna, and P. Skands, JHEP, 0605-026 (2006).
- [14] D.J. Lange, Nucl. Instrum. Methods Phys. Res., Sect. A **462**, 152-155 (2001).
- [15] S. Agostinelli *et al.*, Nucl. Instrum. Methods Phys. Res., Sect. A **506**, 250 (2003).
- [16] E. Farhi, Phys. Rev. Lett. **39**, 1587 (1977).
- [17] E. L. Allwein, R. E. Schapire, and Y. Singer, J. Machine Learning Res. **1**, 113 (2000).